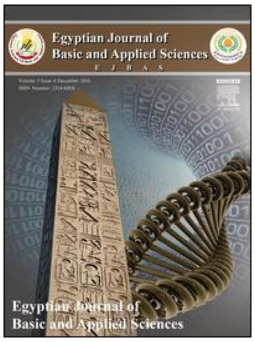

Egyptian Journal of Basic and Applied Sciences

ISSN: (Print) 2314-808X (Online) Journal homepage: https://www.tandfonline.com/loi/teba20

Influence of doping chromium ions on the electrical properties of hydroxyapatite

Moustafa Ibrahim & Abdelfattah Dawood

To cite this article: Moustafa Ibrahim & Abdelfattah Dawood (2020) Influence of doping chromium ions on the electrical properties of hydroxyapatite, Egyptian Journal of Basic and Applied Sciences, 7:1, 35-46, DOI: 10.1080/2314808X.2019.1710055

To link to this article: https://doi.org/10.1080/2314808X.2019.1710055

EGYPTIAN JOURNAL OF BASIC AND APPLIED SCIENCES
2020, VOL. 7, NO. 1, 35–46
https://doi.org/10.1080/2314808X.2019.1710055

Taylor & Francis
Taylor & Francis Group

Influence of doping chromium ions on the electrical properties of hydroxyapatite

Moustafa Ibrahim and Abdelfattah Dawood

Department of Physics, Benha University, Benha, Egypt

ABSTRACT

Hydroxyapatite $Ca_{10}[PO_4]_6[OH]$ is a biocompatible widely used in medicine and dentistry. Its applications depend greatly upon lattice substitution of Calcium sites in its structure by varies cations such as Na, Mg, Sr, Ag etc. Chromium plays an important role in reducing blood sugar level and improving insulin ability to convert glucose in cells to gain energy. In this paper we studied the effect of doping hydroxyapatite with chromium ions on its crystal dielectric properties. Pure hydroxyapatite and chromium loaded hydroxyapatite of chromium concentrations of 0.5, 1.0, 2.0, and 3.0 wt % forming samples S1, S2, S3 and S4 respectively were prepared by wet precipitation method. The dielectric parameters, permittivity $\dot{\varepsilon}$, dielectric loss $\ddot{\varepsilon}$, conductivity σ, relaxation time t_s and dielectric modulus M′ and M′′ were calculated at frequency of 20 Hz to 10 MHz. Results showed increase of $\dot{\varepsilon}$, and $\ddot{\varepsilon}$, values of chromium loaded samples compared to pure hydroxyapatite. The conductivity of the doped samples was increased with chromium concentration increase. The relaxation times (t_s) chromium loaded samples showed increase of t_s as chromium concentration increase. The dielectric properties showed that as chromium concentration increase, $\dot{\varepsilon}$, $\ddot{\varepsilon}$, and σ of substance increase compared to the pure HA.

ARTICLE HISTORY
Received 3 July 2019
Accepted 26 December 2019
Published online 10 January 2020

KEYWORDS
Chromium hydroxyapatite; conductivity; dielectric properties; electric modulus; relaxation time

Introduction

A wide range of research studies have focused on the synthesis and application of hydroxyapatite (HA) on bones. HA, Ca10(PO4)6(OH)2, HA, is well known as biomaterial or bioceramics because of its role in substituting bone and teeth damages [1–3]. Although it has a significant role in bone replacement and substitution, as it forms about 60–70% of human bones [4], its application is limited due to its low brittleness [5,6]. Therefore, several efforts were carried out in order to obtain similar biomaterials which can be used in such a role with a comparably higher order of stiffness with biocompatibility and biodegradability [3, 7]. HA was doped and prepared artificially with several substances such as aluminum, iron, magnesium, zinc, strontium and sodium in order to improve its mechanical and electrical properties.

These doped substances should also have similar properties like the native HA but with improved characteristics like biocompatible as well as application as antibacterial activity [8,9]. Moreover, HA can also be used in bone osteopenia curing and bone damage substituting.

Here, HA is doped with chromium ions (prepared by the wet precipitation method) at four different concentrations (0.5, 1.0, 2.0 and 3.0 wt %) to prepare samples S1, S2, S3 and S4, respectively. It has been reported that chromium concentration becomes low in people with

CONTACT Moustafa Ibrahim mustafa.ibrahim@fsc.bu.edu.eg Department of Physics, Benha University, Benha, Egypt

diabetes, where chromium enhances insulin signaling, reduces insulin resistance and improves carbohydrate metabolism [10–12]. Chromium has been shown to reduce the possibility of suffering from cardiovascular disease [13,14]..

In this work, we investigated the effect of doping chromium ions on the electrical conductivity and dielectric properties of pure HA and chromium HA (S1, S2, S3 and S4) recorded at three different temperatures of 298, 308 and 318 K.

Methods

Chromium hydroxyapatite (Cr-HA) preparation

Calcium phosphate powder was prepared by precipitation method as follows: 0.16 mol of calcium nitrate tetrahydrate [$Ca(No_3)_2 \cdot 4H_2O$] was dissolved in 1 l of de-ionized water and 0.096 mol of di-ammonium hydrogen ortho-phosphate [$(NH_4)_2$ HPO_4] to accomplish the Ca/P ratio at 1.67. The Cr-HA was prepared as follows: different amounts of chromium nitrate Cr $(No_3)_2 \cdot 9H_2O$ [0.005, 0.01, 0.02, 0.03 mol] was dissolved in 1 l of de-ionized water with 0.16 mol of calcium nitrate tetrahydrate [Ca $(No_3)_2 \cdot 4H_2O$]. The pH was adjusted to about 10 by adding dilute NH_4OH solution. A volume of 0.096 mol [$(NH_4)_2HPO_4$] solution was fed from a burette (2–5 ml/min) into a stirred solution of 0.16 mol [$Ca(No_3)_2 \cdot 4H_2O$] heated to 60°C on a hot plate (at pH = 10). Then, the solution was aged and stirred at its boiling point for about 2 h in a sealed container. The pure and Cr-HA samples were obtained by sucking filtration and purified three times with de-ionized water. The product was then dried overnight at 100°C and powdered by grinding mill.

The preparation and characterization methods were published [12].

Dielectric measurements

Samples (2 mg tablets) were prepared for each Cr-HA concentration, S1, S2, S3, S4 and the pure, by compressing to a pressure of 1500 PSI and left for 10 min for homogeneity to form a tablet of diameter of 0.8 cm and thickness of 0.09 cm.

The measurements were conducted using a Novo control High-Resolution Alpha Analyzer using gold-plated stainless-steel electrodes of 20 mm in diameter, in parallel plate capacitor configuration. A Quatro Temperature Controllers using pure nitrogen were used to stabilize the temperature during the experiment

The dielectric measurements were obtained using gold-plated stainless-steel electrodes of 20 mm in diameter. The data acquired include the capacitance (C), resistance (R), impedance (Z) and delay angle (θ). HA doping might generate crystal structure defects and thermal instability as stated by [15]; therefore, the experiment was conducted at different temperatures of 298, 308 and 318 K.

The acquired data were used to calculate dielectric properties using the following equations:

$$\varepsilon' = \frac{cd}{\varepsilon_0 A} \quad (1)$$

$$\varepsilon'' = \varepsilon' \tan\delta \quad (2)$$

$$\tan\delta = \tan(90 - \theta) \quad (3)$$

Complex impedance data, Z*, can be represented by its real, Z′, and imaginary, Z″, parts by the following relation:

$$Z* = Z' + jZ \quad (4)$$

Using complex impedance, the real and imaginary parts of the complex impedance of the equivalent circuit can be written as

$$z' = z \cos\theta \quad (5)$$

$$z'' = z\, sin\theta \quad (6)$$

$$\sigma = \frac{d}{A} \times \frac{1}{R} \quad (7)$$

where σ is the electric conductivity, A is the area of electrode in m^2, d is the distance between the two electrodes in m, ε′ is the dielectric permittivity and ε′′ is the dielectric loss.

The measured parameters were used to calculate both parts of the dielectric permittivity, the real ε′ and imaginary ε′′, real and imaginary parts of conductivity, σ′ and σ″, respectively (measured in S/m), real and imaginary parts of impedance, Z′ and Z″, respectively (in ohm).

ε′ and ε′′ data were used to calculate the real and imaginary part of electric modulus, M′ and M′′ formalisms.

$$M^* = M' + jM'' \tag{8}$$

$$= \frac{\varepsilon'}{\varepsilon'^2 + \varepsilon''^2} + j\frac{\varepsilon''}{\varepsilon'^2 + \varepsilon''^2} \tag{9}$$

where M′ and M″ are the real and imaginary parts of electrical modulus, respectively.

Relaxation time was calculated from the Cole–Cole semicircles (Nyquist plot) from the following relation:

$$\omega_s = \frac{2\pi}{\tau_s} \tag{10}$$

where ω_s is the angular frequency and τ_s is the relaxation time.

Results and discussion

The dielectric parameters of the pure and Cr-HA samples (S1, S2, S3 and S4) with different concentrations (0.5, 1.0, 2.0 and 3.0 wt. %) respectively,, were measured at different temperatures (298, 308 and 318 K) and plotted against applied frequency. The results of the dielectric properties of the Cr-HA show a relatively higher activity of doped samples compared to the pure one.

Figure 1 represents the relation of the real part of the dielectric permittivity (ε′) as a function of the frequency which shows increasing in ε′ values as chromium concentration increases apart from S4. Values of ε′ of the pure HA, at low frequencies, are the lowest and those of chromium loaded(S1 and S2) are comparable and S3 and S4 are relatively high. All samples show similar values at high-frequency range. This is attributable to the gradual formation of the chromium crystals inside the structure of HA [16]. Surprisingly, S3 shows the highest values of ε′ compared to the rest including S4.

As temperature increases from room temperature the overall values of ε′ increased, and yet S3 had the highest values. Where, as the concentration of the doped as chromium concentration increase, the amount of dipole inside samples also increase which lead to higher permittivity. At high frequencies, dipoles hardly follow the alternating electric filed therefore data exhibit dielectric relaxation of all Cr-HA samples with decreasing dielectric constant [17]. At chromium concentration higher than 0.2% (i.e. S4), the increased concentration seems to affect the dipole polarization which resulted in a reduction in ε′ values and it could be attributed to interfacial polarization [18]. Also, sample-electrode has poor-contact interaction which resulted in grain boundary formation which also would affect the values ε'.

All samples behave similarly at high frequency, particularly values at a frequency higher than 1 kHz. Raising sample temperature insignificantly influenced the dielectric values at higher frequencies, while it did at low frequencies .

Nyquist plots at temperature changes – 298, 308 and 318 K

Nyquist plots of the samples under investigation were established using the Z view software (a software program set to plot and simulate Z′ and Z″ data to an equivalent RC circuit).

All samples show more than one semicircle which can be due to the formation of grain boundary charges between samples and used electrode.

The pure HA sample showed formation of grain boundary (represented by sub-semicircle) greater than samples S1, S2, S3 and S4 represented by the small semicircle at low frequency.

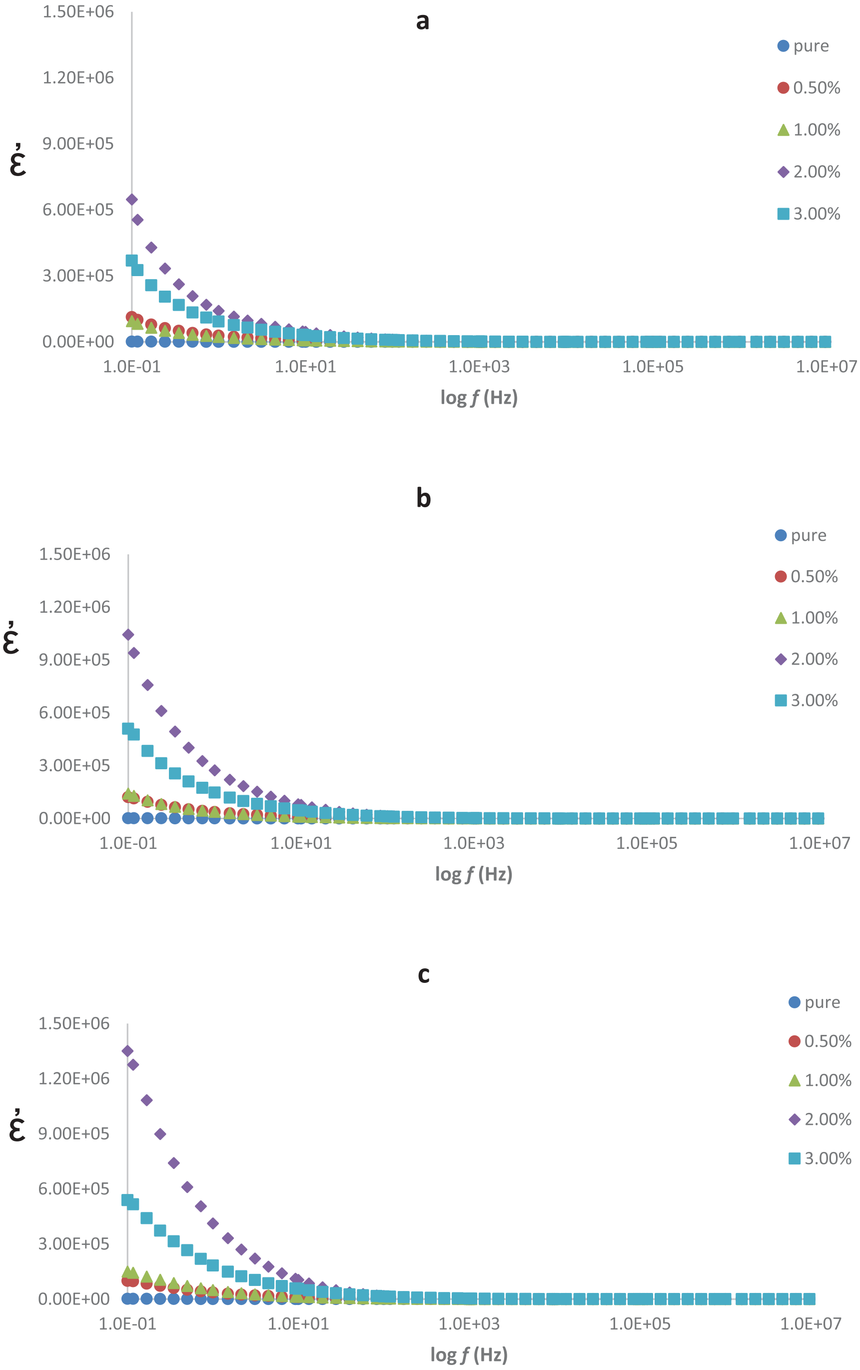

Figure 1. The dielectric constant (ε′) as a function of frequency (0.1–100 Hz) for the pure and Cr-HA samples S1, S2, S3 and S4 at temperatures of (a) 298 K, (b) 308 K and (c) 318 K, respectively.

Sample S4 at chromium concentration of 3.0% (Plot 2E) showed another small sub-semicircle at very low frequencies. It showed three semicircles indicating more resistance and more relaxation regions at very low-frequency regions between electrode and charges accumulated in the sample. This could be due to sample–electrode poor contact region between sample and electrode which results in a higher capacitive impedance (i.e. lower capacitance and consequently lower dielectric permittivity).

Therefore, S3 is the best highest chromium concentration that can be used, especially the values of dielectric constant, as illustrated in Figure 2, and impedance of S3 are very much comparable to that of S4 and both are significant form other samples.

Data obtained from the above plots are tabulated in Table 1. This table represents the resistance, capacitance of the equivalent circuit as well as the dispersion angle of the semicircle center beneath the x-axis and finally the relaxation time of the dipole to return to thermal equilibrium from Equation7.

Data show that all samples are comparable at low-frequency regions and also fluctuate at high-frequency regions in almost all parameters with no significant differences, except relaxation time.

Relaxation time at low-frequency regions is much lower than that of the high-frequency regions at all samples. Relaxation time of S3 at the applied temperature range, at low- and high-frequency regions, shows the fastest of all (smaller values). This could be due to optimum dipole orientation at the applied frequencies compared to the rest.

The increased values of R, C and τ_s could be due to the bonds broken between HA compositions.

To manifest the differences between samples at the applied temperatures, dielectric constant ε′ was plotted versus frequency at a low range. All chromium-loaded samples show better dispersion (separation between curves) than pure HA, and S3 showed the best of all.

The AC conductivity of the Cr-HA at different temperatures is illustrated in Figure 3 and Figure 4. It shows similar behavior in pure HA and Cr-HA samples, S1, S2, S3 and S4 as sample temperature rise from (298–318 K). However, values of the Cr-HA samples are quite higher than that of the pure HA. Generally, The trend of AC conductivity shows no major change between the AC conductivity values at (298K) and (318K).This contributes to the idea that there are no major differences between samples under investigations under the applied temperature from 298 to 318 K), i.e. samples are stable under this small temperature increment.

In general, AC conductivity values increase at lower frequencies as chromium concentration increases, which is related to the interaction of the doped chromium ions with HA, which affects conductivity positively. However, at higher frequencies, the electrical conductivity displays quite similar values, especially for higher chromium concentrations S3 and S4, which can be attributed to the reduction in pores and interspaces for chromium ions, which reduced the conductivity [19].

In order to optimize the electrode polarization effect, the modulus values (M′ and M′′) are plotted for the pure and Cr-HA at a temperature of 298 K (Figure 5).

Curves show increase of M′′ as M′until saturates to form a peak at approximately the middle of M′ data (at high frequency), then decreases as M′ increases (at very high-frequency region). Moreover, the peak is shiftedtowards low frequency and decreases in value as chromium concentration increase which is due to transition from short to long range mobility as chromium concentration increase at low frequency region as illustrated previously in Nyquist plots (Figure 2) [20].

Real part of modulus (M′) values are plotted in Figure 6. At low frequencies, the values of M′ are very low, indicating suppression of electrode polarization [21], where, all polarization processes, i.e. the electronic, ionic, dipolar and surface polarization, could be attributed in terms of modulus M′ at low frequencies.

Higher values of M′ correspond to higher frequencies, which in turn correspond to lower values of M′′, indicating polarization reduction [22].

As chromium concentration increases, M′ values shifted to higher frequencies with

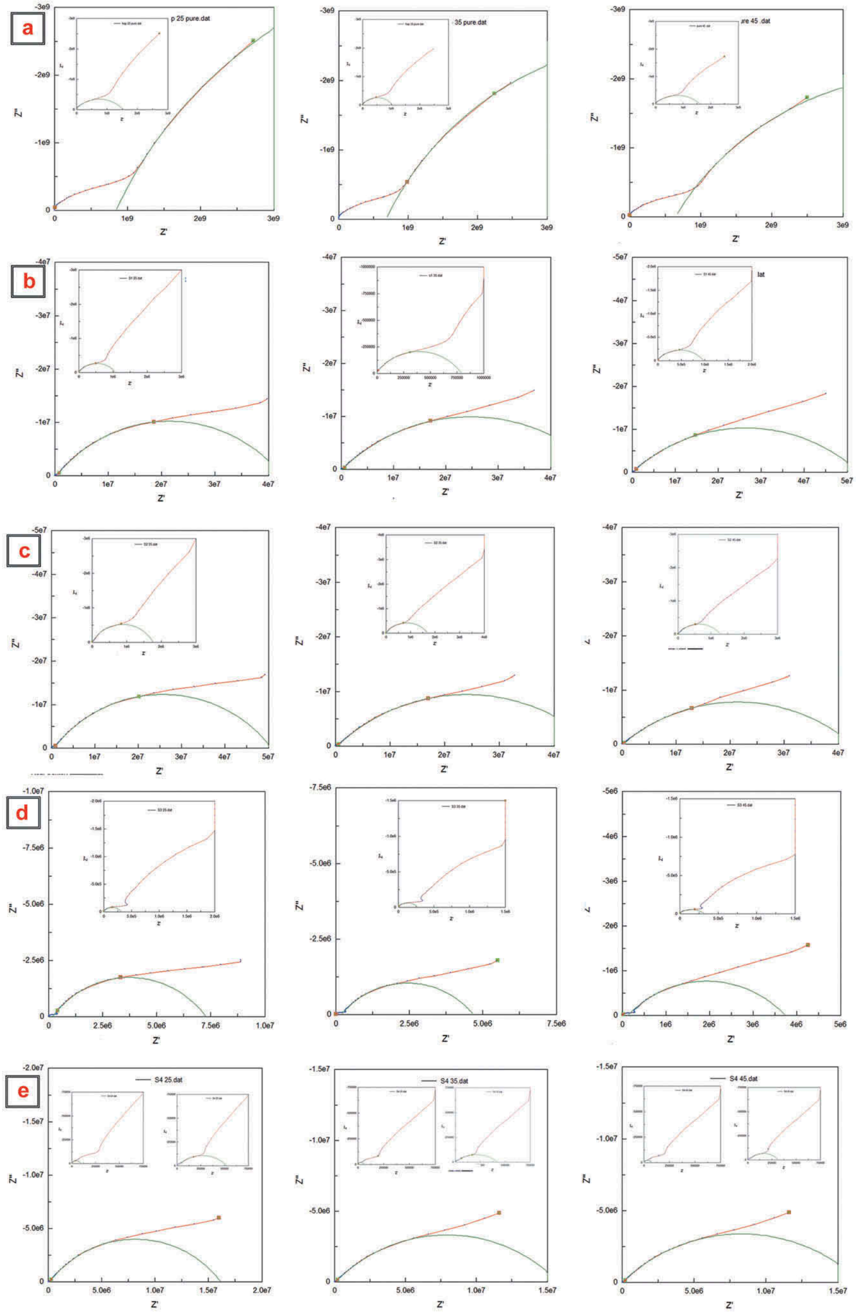

Figure 2. Nyquist plot (Z′ vs Z″) of the pure (a) and chromium HA S1 (b), S2 (c), S3 (d) and S4 (e), at temperatures of 298, 308 and 318 K. Main plot represents semicircles at high frequencies (full range), while the semicircles at low frequencies (low and very low) are represented by the sub-figure in each plot.

lower values of M′, which is attributed to chromium concentration effect.

M″ showed low values and it relatively increased as frequencies increased until it reaches its maximum value at the maximum frequency f_{max} and then it relaxes to lower values as frequency increases as illustrated in Figure 7.

Table 1. The RC equivalent circuits' parameters: resistance, capacitance, relaxation times and depression angles of pure and Cr-HA samples at high-frequency (full) and low-frequency (low and very low) ranges.

1-Pure HA

	R (ohms)		C (Farad)		Relaxation time τ_s (sec)		Depression angle α	
Temperature	Low	full	Low	full	Low	full	Low	full
298 K	9.88E5	4.10E7	9.57E-12	6.10E-9	7.29E-05	1.99	35.33	37.76
308 K	1.66E5	4.82E7	2.77E-11	4.73E-09	3.26E-04	1.78	26.81	36.53
318 K	9.42E5	7.41E7	7.21E-12	5.79E-10	5.26E-03	5.23	35.78	30.50
2-S1								
298 K	1.09E6	4.23E7	9.97E-12	5.72E-9	8.60E-05	1.94	37.49	38.34
308 K	8.04E5	4.92E7	9.35E-12	1.25E-8	5.80E-05	5.59	35.50	46.06
318 K	9.99E5	5.27E7	9.79E-12	1.44E-8	8.10E-05	7.31	40.70	47.21
3- S2								
298 K	1.76E6	5.02E7	2.76E-11	4.83E-9	3.49E-04	1.92	28.73	37.44
308 K	1.72E6	4.74E7	3.94E-11	1.18E-8	5.40E-04	5.13	37.59	46.48
318 K	1.28E6	4.24E7	3.51E-11	2.27E-8	3.66E-04	9.34	39.31	49.54
4- S3								
298 K	3.19E5	7.12E6	4.7E-12	1.49E-8	1.15E-5	0.84	34.35	37.74
308 K	3.73E5	4.49E6	4.71E-12	3.95E-8	1.66E-5	1.46	48.58	40.03
318 K	3.39E5	3.61E6	4.2E-12	8.08E-8	1.49E-5	2.54	52.67	43.89

5- S4

	R (ohms)			C (Farad)			Relaxation time τ_s (sec)			Depression angle α		
Temperature	Very low	Low	full	Very low	Low	full	Very low	Low	full	Very low	Low	full
298 K	71564	5.15E5	7.12E6	3.35E-12	3.34E-11	1.49E-8	2.46E-6	1.51E-4	2.10	26.63	44.49	36.98
308 K	62375	4.27E5	1.57E7	2.98E-12	3.77E-11	1.57E-7	1.25E-6	1.60E-4	5.12	21.36	50.88	44.15
318 K	81658	3.06E5	1.66E7	3.04E-12	2.63E-11	3.46E-8	1.83E-6	6.83E-5	5.18	31.65	42.41	45.67

The values of f_{max} shifted to a higher frequency region with increasing chromium-doping concentration, i.e. chromium distribution in HA lattice. f_{max} peaks of M″ are shifted from 763 Hz at pure HA to higher frequencies (~1.5–~5 MHz) as chromium concentration increases as illustrated in S1–S4 (Table 2). This signifies the effect of chromium concentration on the structure of calcium HA, and this effect is accumulated as chromium concentration increases.

Conclusion

Calcium HA was doped with small amount of chromium ion concentration from 0.5 to 3% wt to study the effect of Chromium-Calcium substitution on its AC conductivity and dielectric properties.

Results show that as chromium concentration increases, the electrical conductivity increases, indicating a better biocommunication of Cr-HA compared with the pure HA. The dielectric permittivity of the HA crystal at low frequencies increased with increasing chromium-doping concentration, while all samples, the pure and doped ones, show a relatively comparable trend at higher frequency region. HA-doped sample at a concentration of 2% wt showed the best dielectric behavior, the least resistance and the highest relaxation frequency and showed the fastest relaxation time (as estimated from the Nyquist semicircles) at low-frequency and high-frequency regions under the applied temperature. The electrical conductivity and dielectric properties increased as temperature increases, which means that chromium ions doping improve HA bioconductivity and enhances its electrical properties.

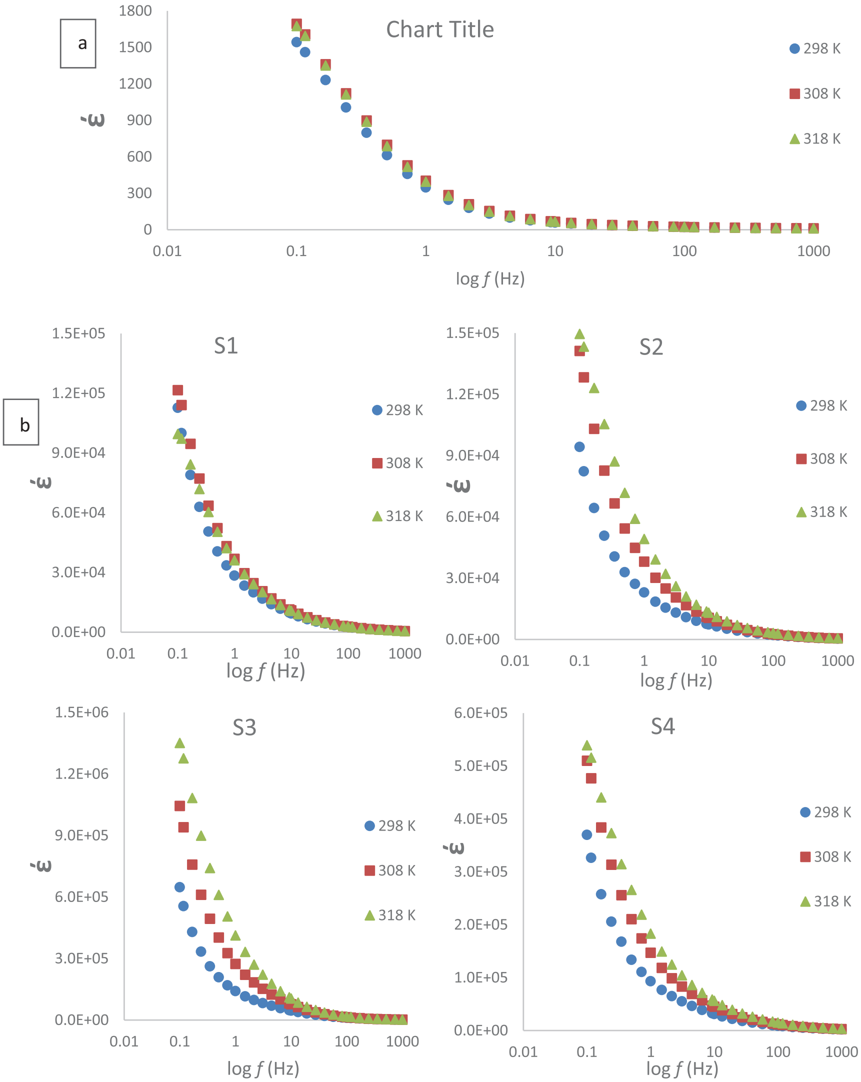

Figure 3. Comparison of the dielectric constant (ε′) at temperatures 298, 308 and 318 K at low-frequency range (0.1–1000 Hz), in logarithmic scale, for the hydroxyapatite; pure (a) and chromium-loaded {S1, S2, S3 and S4 (b)}.

The maximum frequency that is correlated with a dipole relaxation time of Cr-HA samples is higher than that of the pure HA and it increases as chromium concentration increases and decreases again at S4.

These findings support the fact that the substitution of chromium ions in the Ca-HA crystal influenced its electrical properties, permittivity, conductivity and dipolar relaxation time, which means it can be used for dental and bone treatments.

Acknowledgments

I would like to thank professor Dr Samira Sallam, Physics department, Faculty of science, Benha University, Egypt, for her help in paper discussion and Dr Faten Adel for providing the samples.

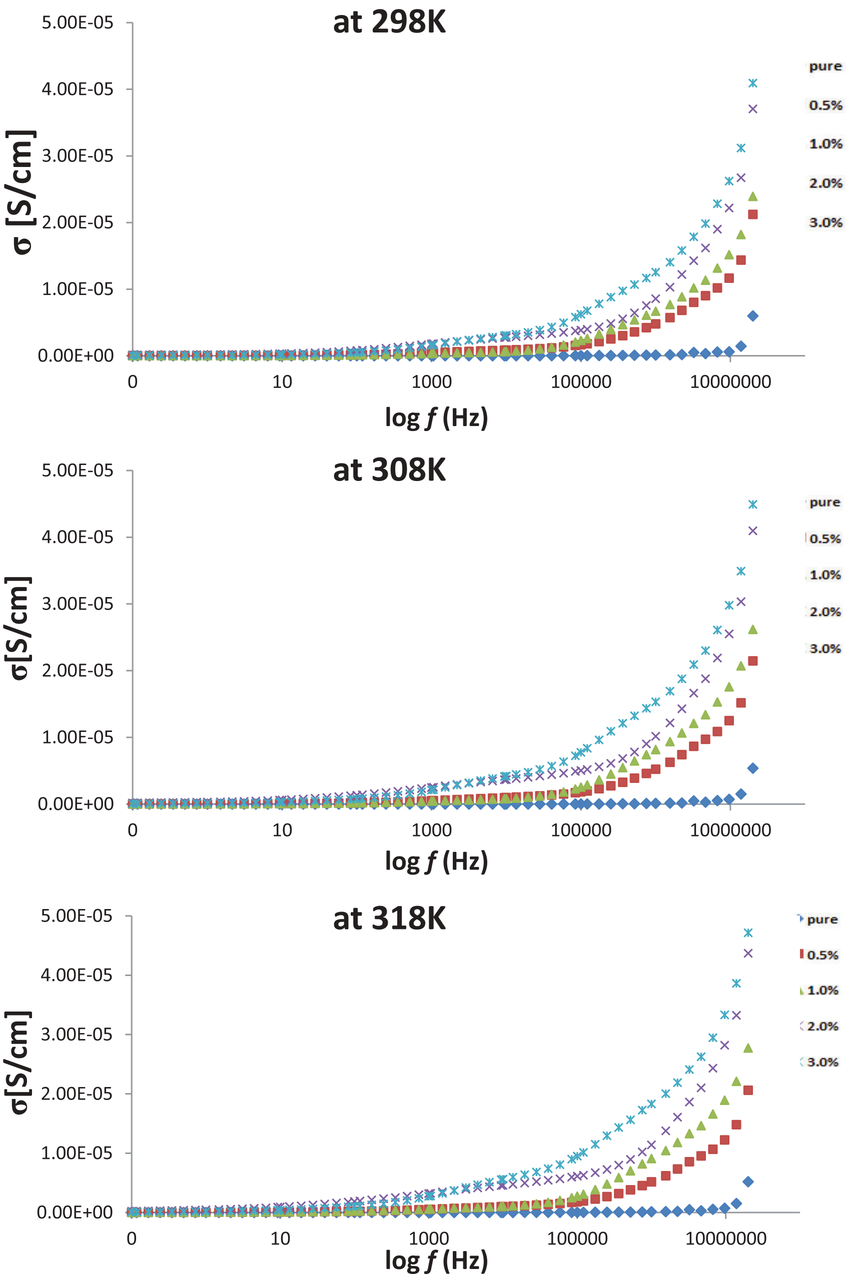

Figure 4. AC electrical conductivity (σ) as function of frequency (at logarithmic scale) for the pure and Cr-HA samples S1, S2, S3 and S4 at temperatures 298, 308 and 318 K.

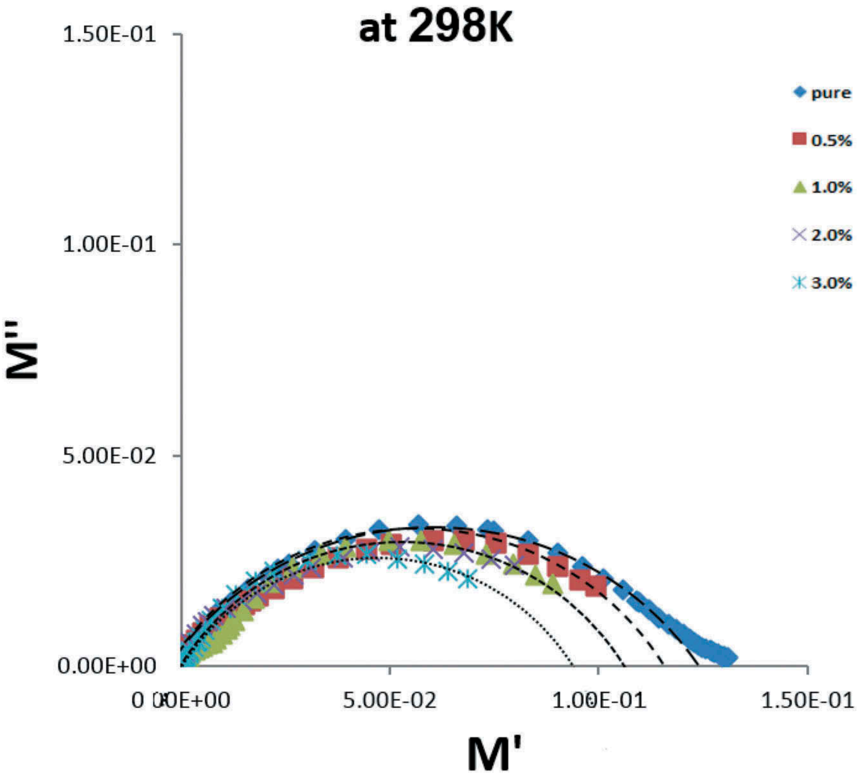

Figure 5. Real and imaginary parts of dielectric modulus (M′ and M″), respectively, as a function of frequency at temperature 298 K.

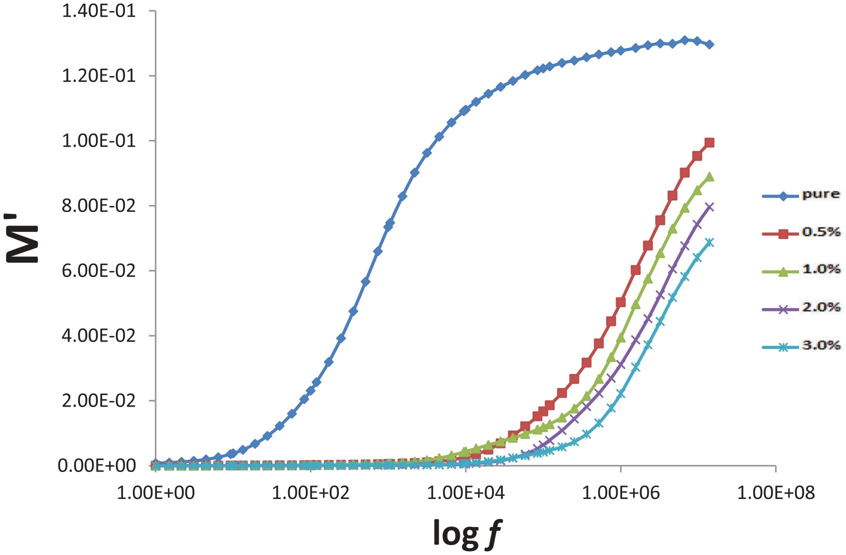

Figure 6. The real parts of dielectric modulus M′ as a function of frequency at the temperature of 298 K.

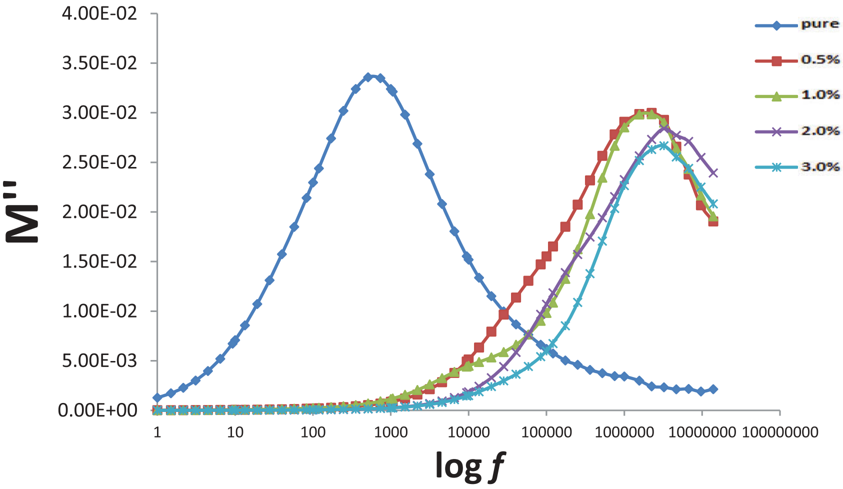

Figure 7. The imaginary parts of dielectric modulus M″ as a function of frequency at room temperature.

Table 2. The values of average maximum frequency f_{max} for HA pure and Cr-HA (S1, S2, S3 and S4) of chromium concentrations (0.5, 1.0, 2.0 and 3.0 wt%), respectively.

Sample	f_{max} (MHz)
Pure	7.63×10^{-4}
S1	1.56
S2	2.4
S3	4.65
S4	3.23

Disclosure statement

No potential conflict of interest was reported by the authors.

ORCID

Moustafa Ibrahim http://orcid.org/0000-0002-2580-027X

References

[1] Pryor L, Gage E, Langevin C-J, et al. Review of bone substitutes. *Craniomaxillofacial Trauma Reconst*. 2009;2(03):151–160.

[2] Prakasam M, Locs J, Salma-Ancane K, et al. Fabrication, properties and applications of dense hydroxyapatite: a review. J Funct Biomater. 2015;6(4):1099–1140.

[3] Denes E, Barrière G, Poli E, et al. Commentary: bioceramics and scaffolds: a winning combination for tissue engineering. Front Bioeng Biotechnol. 2017;5(December):1–17.

[4] Walters MA, Leung YC, Blumenthal NC, et al. A Raman and infrared spectroscopic investigation of biological hydroxyapatite. J Inorg Biochem. 1990;39(3):193–200.

[5] Suchanek W, Yashima M, Kakihana M, et al. Hydroxyapatite ceramics with selected sintering additives. Biomaterials. 1997;18(13):923–933.

[6] Rogina A, Antunović M, Milovac D. Biomimetic design of bone substitutes based on cuttlefish bone-derived hydroxyapatite and biodegradable polymers. J Biomed Mater Res Part B. 2017. DOI:10.1002/jbm.b.34111

[7] Ibrahim M, Sallam S.Egypt. J. Biomed. Eng. Biophys. 2018;19:1.

[8] Bajpai I, Saha N, Basu B. Moderate intensity static magnetic field has bactericidal effect on E. coli and S. epidermidis on sintered hydroxyapatite. J Biomed Mater Res Part B. 2012;100B(5):1206–1217.

[9] Ciobanu CS, Iconaru SL, Le Coustumer P, et al. Antibacterial activity of silver-doped hydroxyapatite nanoparticles against gram-positive and gram-negative bacteria. Nanoscale Res Lett. 2012;7:1.

[10] McCarty MF. Anabolic effects of insulin on bone suggest a role for chromium picolinate

in preservation of bone density. Med Hypotheses. 1995;45(3):241–246.

[11] Chen W-Y, Chen C-J, Liu C-H, et al. Chromium supplementation enhances insulin signalling in skeletal muscle of obese KK/HIJ diabetic mice. Diabetes Obes Metab. 2008;11:293–303.

[12] Sallam SM, Tohami KM, Sallam AM, et al. Synthesis and characterization of hydroxyapatite contain chromium. J Biophys Chem. 2012;3(4):278–282.

[13] Anderson RA, Polansky MM, Bryden NA, et al. Supplemental-chromium effects on glucose, insulin, glucagon, and urinary chromium losses in subjects consuming controlled low-chromium diets. Am J Clin Nutr. 1991;54(1):909–916.

[14] Wilson BE, Gondy A. Effects of chromium supplementation on fasting insulin levels and lipid parameters in healthy, non-obese young subjects. Diabetes Res Clin Pract. 1995;28 (3):179–184.

[15] dos Santos MG, Barbosa NS, Resende XR,et al. Mater. Res. 18 881 (2015).

[16] Zhao H, Xia YJ, Dang ZM, et al. Composition dependence of dielectric properties, elastic modulus, and electroactivity in (carbon black-BaTiO3)/silicone rubber nanocomposites. J Appl Polym Sci. 2013;127(6):4440–4445.

[17] Kar SK, Kumar P. Permittivity and modulus spectroscopic study of BaFe 0. 5 Nb 0. 5 O 3 ceramics. 2013 P. 181–187. DOI: 10.2298/PAC1304181K.

[18] Gregorio R. J. Appl. Polym. Sci; 2002: 752.

[19] Hu S, Li Y-F, Yang R, et al. Structure and ionic conductivity of Li7La3Zr2−xGexO12 garnet-like solid electrolyte for all solid state lithium ion batteries. Ceram Int. 2018;44(6):6614–6618.

[20] Liu J, Duan CG, Yin WG, et al. Dielectric permittivity and electric modulus in Bi2Ti4O11. J Chem Phys. 2003;119(5):2812–2819.

[21] Afandiyeva IM, Bülbül MM, Bengi S. Microelectronic engineering frequency dependent dielectric properties and electrical conductivity of platinum silicide/Si contact structures with diffusion barrier. Microelectron Eng. 2012;93:50–55.

[22] Aziz SB. The mixed contribution of ionic and electronic carriers to conductivity in chitosan based solid electrolytes mediated by CuNt Salt. J Inorg Organomet Polym Mater. 2018;1–11. DOI:10.1007/s10904-018-0862-3